"Contact Voltage" in Nanoparticle/Molecule Connections

H. Modrow,*,† S. Modrow,†,⊥ J. Hormes,‡ N. Waldöfner,§ and H. Bönnemann||

Physikalisches Institut der Universität Bonn, Nussallee 12, 53115 Bonn, Germany, Center for Advanced Microstructures and Devices, 6980 Jefferson Highway, Baton Rouge, Louisiana 70806, MagForce Applications GmbH, Spandauer Damm 130, 14050 Berlin, Germany, and Max Planck Institut für Kohlenforschung, Kaiser-Wilhelm Platz 1, Mülheim a.d. Ruhr, Germany

Received: July 20, 2004; In Final Form: October 22, 2004

This work presents conclusive evidence that connecting Pt and Co nanoparticles stabilized by an aluminum-organic shell with molecular spacers interacting with this shell can induce notable changes in the electronic structure of the metal. X-ray absorption spectroscopy measurements at the Al K-, the Pt L_{III}-, and the Co K-edge provide consistent evidence for this effect. The changes induced by cross-linking with an acidic spacer are discussed in detail as an example to elucidate the mechanism of this effect. It turns out that a reconfiguration of the protection shell that occurs upon networking is responsible for the observed changes.

Introduction

One of the prospects and hopes connected with the recent efforts in the field of nanotechnology and the progress rewarding these efforts is the miniaturization of optical and electronic devices. At the same time, each step in this miniaturization process brings us closer to the quantum regime, where it is well known that the connection of a system in a well-defined state to the outside world, as it occurs, for example, during a measurement process, disturbs that state. Consequently, the question arises whether/under which conditions the nanoelectronic device will remain intact when integrated into a circuit. For "molecular" electronics systems as discussed, for example, in refs 1−5, such effects have been investigated recently by Cui et al.,[6] who also suggest another example where this effect may be found: Following different author's opinions,[7−10] DNA behaves as a conductor, semiconductor, or insulator or shows superconducting properties, and in fact these contradictions appear plausible if one assumes that the "wiring" in the specific experimental setup has an influence on the electronic structure of the molecule.

Recently, several studies have demonstrated considerable sensitivity of the properties of nanoparticle cores with respect to the coordination chemistry of the surrounding matrix. For example, Vestal and Zhang[11] investigated the effect of surface coordination chemistry on magnetic properties of $MnFe_2O_4$ spinel ferrite nanoparticles; a detailed and concise attempt to explain the reason for these changes is presented for a series of substituted bezoic acid and benzene ligands, in which the role of the specific group coordinating to the nanoparticle is stressed. Torma et al. showed that the activation energy for electron transfer between covalently linked Au clusters is dependent on the electronic nature of the linking molecules.[12] Another series of studies[13−16] has shown that electron relaxation dynamics after femtosecond laser excitation in nanoparticles is a function of the embedding medium. In particular, for example, Link et al.[16] have compared the plasmon band bleach recovery of electrochemically synthesized gold nanoparticles of 14.5 and 21 nm size embedded in $MgSO_4$ powder and solution, respectively. Surprisingly, they find that the fast decay component, which is usually ascribed to the electron−phonon relaxation inside the gold nanoparticles, is dependent on the environment of the particles.

These mostly indirect indications for changes in the electronic structure, which are also not just limited to metal systems,[17−19] are fully backed by a number of theoretical and experimental results using a technique which probes electronic and geometric structure directly: X-ray absorption spectroscopy. Rehr et al.[20] have predicted significant changes in the spectra of small Pt clusters upon hydrogen adsorption on the basis of theoretical calculations. Horokawa et al.[21] correlate changing optical properties of CdS nanoparticles and changes in the solvated surface structure of these particles. Zhang and Sham have pointed out that the electronic properties of gold nanoparticles can be manipulated by suitable choice of capping molecules[22] and recently demonstrated that size-variation and surfactant-influence for such particles are intertwined.[23] The authors of this work detected surfactant-dependent influence on the electronic structure of Pd nanoparticles,[24] which was confirmed and backed by a detailed model for this behavior on Co samples.[25]

The purpose of this study was to clarify whether, as in the molecular case mentioned at the beginning of this Article, changes induced in the surfactant shell of the nanoparticle when it is connected to a molecular linker by a reaction in the protection shell in a second reaction step can influence the electronic properties of the particle itself significantly, just as a contact voltage can appear when connecting different metals in a circuit. In addition, this issue is of crucial importance because such an approach is frequently used for functionalization of a nanoparticle. Our sample system consists of Al-organically stabilized Pt- and Co-particles; in fact, it should be noted that this protective shell acts as an insulator and the term "contact voltage" is used only in the sense of a familiar example for contact-induced changes in electronic properties. This stabilizer

* Corresponding author. E-mail: modrow@physik.uni-bonn.de.
† Physikalisches Institut der Universität Bonn.
‡ Center for Advanced Microstructures and Devices.
§ MagForce Applications GmbH.
|| Max Planck Institut für Kohlenforschung.
⊥ Present address: Westphal, Mussgnug&Partner, Patent Attorneys, Am Riettor 5, 78048 Villingen-Schwenningen, Germany.

10.1021/jp046787n CCC: $30.25
Published on Web 12/07/2004

SCHEME 1: Synthesis of Nanoparticles with a Pt Core and an Aluminum-Organic Stabilizing Shell

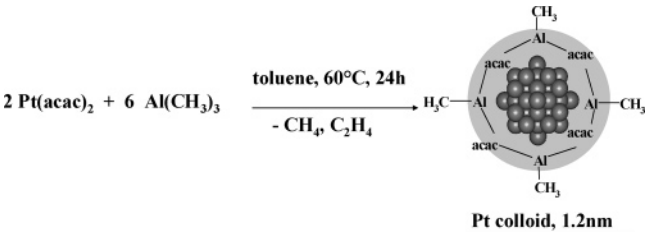

leaves the opportunity to modify the protection shell via substitution of remaining alkyl-groups by OH-groups, which in turn can be used as "connectors" for various types of OH-terminated spacers. The general principle for the synthesis of this type of particles is reported in ref 26; verification of the successful networking of such particles was obtained indirectly in the same paper using a combination of photon and electron spectroscopies. In addition, direct evidence for the network formation has been gained using anomalous small-angle X-ray scattering techniques.[27]

Experimental Section

Sample Preparation. For the preparation of the unconnected Pt samples, 1.97 g of $Pt(acac)_2$ was dissolved under argon atmosphere in 200 mL of dry toluene. 1.44 g of $Al(CH_3)_3$ was dissolved in 200 mL of toluene and carefully added over 24 h at 40 °C. After the gas evolution had stopped, all volatile components were completely evaporated in vacuo. In the residue, 2.4 g of colloidal platinum was obtained in the form of black, air-sensitive powder with a platinum content of 40%. According to protonolysis with acetic acid, six $Al-CH_3$ groups per platinum are present.

A sketch of the particle obtained by this first reaction step is displayed in Scheme 1. Note that in this picture the only intended statement with respect to the nature of the shell is that Al atoms are coordinated to methyl- and acetylacetonate groups simultaneously. A more detailed concept of the local environment of the Al atoms is presented later and visualized in Scheme 3.

The principles of the synthesis of the Co colloids are described in ref 28. In this case, 2.4 g of trioctylaluminum was mixed with 300 mL of toluene and heated to reflux temperature (130 °C). Next, 5.5 g of dicobaltoctacarbonyl was added under vigorous stirring, and the reflux temperature was maintained for 5 h to complete the thermolysis of the carbonyl complex. The resulting black solution was filtered off, and the solvent was evaporated at 40 °C/0.3 Pa. The black, viscous residue was strongly magnetic.

For the synthesis of the networked samples, 0.61 g of the colloidal platinum powder obtained as described above was dissolved in 200 mL of dry tetrahydrofuran (THF). Next, 1.23 g of decanedioic acid (sebacylic acid) was dissolved in 200 mL of THF and added dropwise to the colloidal solution. The mixture was stirred overnight at ambient temperature. The network precipitated and was filtered and washed with THF to remove excess spacer molecules. The result of this reaction step is displayed in Scheme 2. The same procedure was performed with 1.23 g of Co colloid in 400 mL of THF, using 0.3 g of sebacylic acid dissolved in 200 mL of THF to obtain the networked Co particles.

X-ray Absorption Spectroscopy. The XAS spectra were measured in transmission mode at the double crystal monochromator beamline at the Center for Advanced Microstructures and Devices (CAMD) at a storage ring energy of 1.3 GeV for Al and Co measurements and 1.5 GeV for Pt measurements. The experimental setup at this beamline is described elsewhere in detail;[29] YB_{66}(400), Ge(220) and Si(400) crystals were used for monochromatization. The X-ray absorption near edge structure (XANES) spectra were taken with energy steps of 0.09, 0.31, and 0.47 eV at the Al K-, Co K-, and Pt L_{III}-edge, respectively; for extended X-ray absorption fine structure (EXAFS) measurements, steps of about 2.5 eV were chosen, using integration times of 500 ms per data point. Data treatment of the XANES spectra consisted of linear background subtraction in the preedge region and calibration relative to the first inflection point of the corresponding metal reference foil, which was assigned to the energy given in the X-ray data booklet[30] as the corresponding electron binding energy. EXAFS analysis was performed using the UWXAFS package.[31−33] The scattering paths used in the fit were created using the FEFF8 code,[34] based on distance values for Pt foil, PtO_2, and PtAl, respectively.

SCHEME 2: Networking the Individual Nanoparticles with Spacer Molecules (Sebacylic Acid)

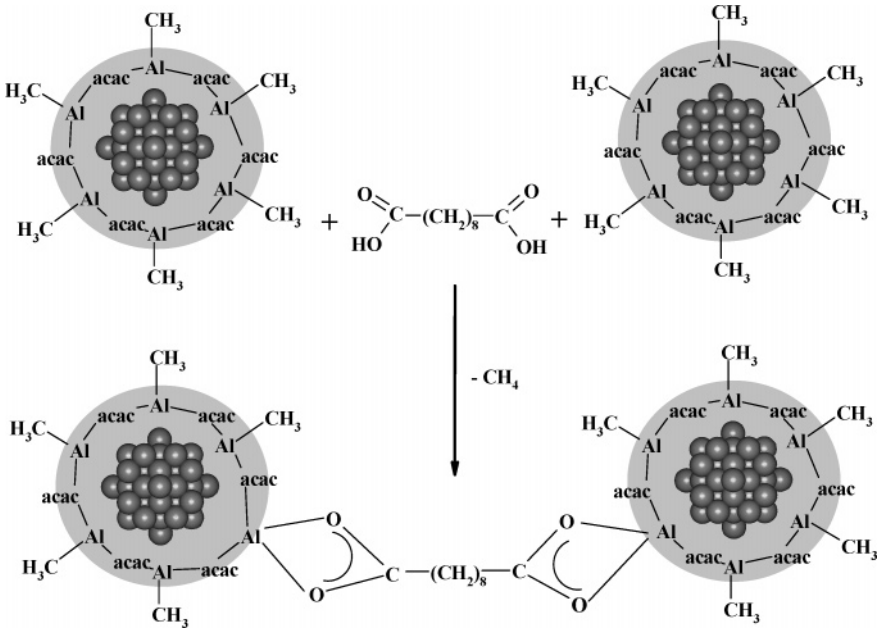

SCHEME 3: Model for the Coordination Geometry of Aluminum Atoms (Marked Al) in the Particle Shell before (Left) and after (Right) Cross-Linking[a]

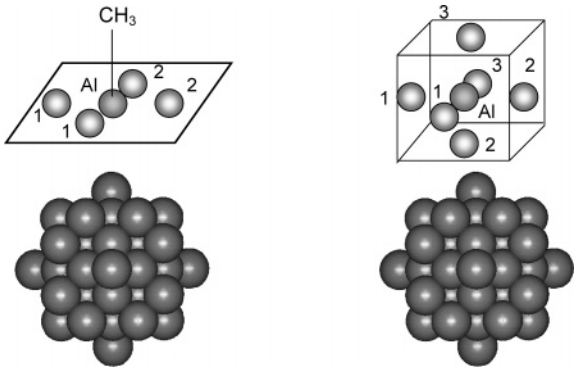

[a] Before cross-linking, there is a more or less planar four-fold oxygen-coordination to O atoms belonging to two different acetylacetonate groups (marked 1 and 2, respectively). After cross-linking, this is transformed into an octahedral coordination suggested by the Al K-XANES data, as two oxygen atoms belonging to the sebacylic acid (marked 3) connect to the Al. As a consequence, oxygen atoms are now found in closer vicinity to the particle surface, as detected by Pt XANES and EXAFS.

Samples were prepared under argon atmosphere in a glovebox, transferred to the beamline under argon using a special airtight sample holder described in detail in ref 35, and measured under argon. An exception from this was made for the Al K-egde, where He was used due to its smaller absorption cross section for 1.5 keV photons. For Pt L_{III}-edge measurements, sample preparation procedures are described in ref 26 for Co K-edge measurements in ref 25. Sample preparation for Al K-edge measurements consisted of distributing a very thin layer of material evenly on 6 μm thick polypropylene foil, relying on adhesive forces to keep the material in place. It should be noted that crystalline reference materials need to be carefully ballmilled to make this preparation approach feasible.

Results and Discussion

Figure 1 shows TEM images of the free platinum-colloids (a) and the network formed after cross-linking of the particles with sebacylic acid (b). The analysis of the average particle size yields 1.3 nm for the free colloids and 1.2 nm for the networked particles, which is identical within the error margins of the analysis.

Figure 2 shows the Pt L_{III} XANES spectra of Pt particles with an aluminum-organic protection shell with a size of about 1.2 nm with and without connecting sebacylic acid spacer molecules in comparison to a Pt foil sample. Whereas the spectra confirm that the geometric structure of the Pt nanoparticles forming the core of the system stays rather similar, as indicated by the high degree of similarity between the shape resonances in the respective spectra, clear differences in the electronic structure are observed. As demonstrated using FEFF8[34] calculations in ref 36, absorption at the energy position at about 11574 eV seems to be characteristic for the presence of a coordinative Pt−Al "bond", whereas the increase in white line intensity is characteristic of oxidative processes and coordination to more electronegative binding partners. Therefore, on the basis of XANES spectra, one would assume that in the networking process at least partly the aluminum-coordination of the particle is substituted by oxygen-coordination. It should be noted that the absorption edge of the interconnected particles is shifted about 1 eV to lower energies. This result suggests that no

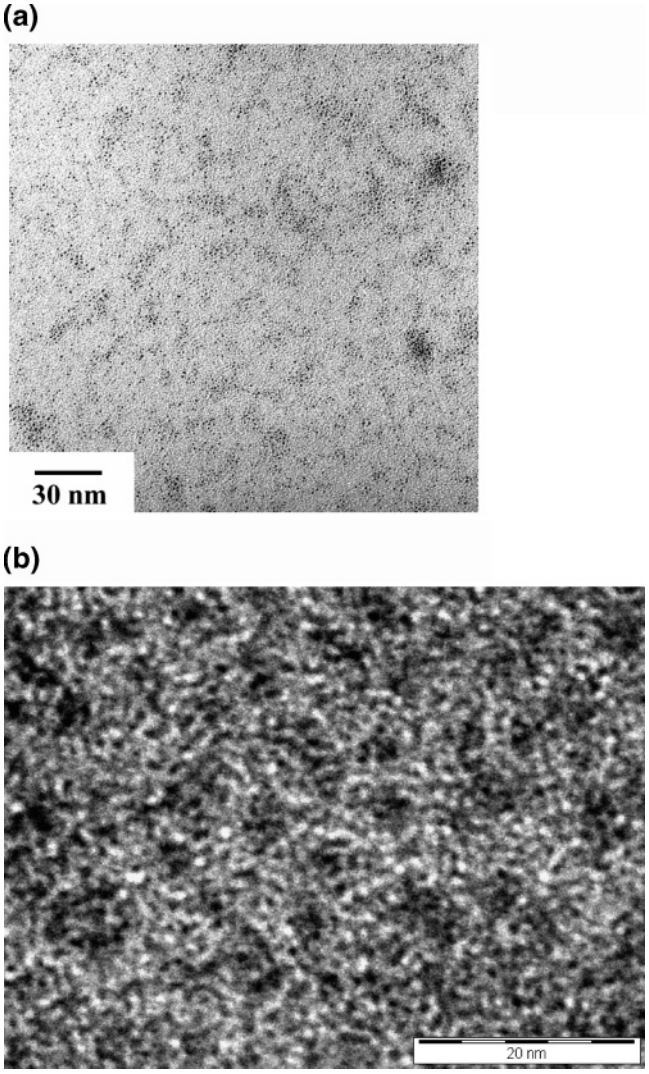

Figure 1. (a) Typical TEM picture of colloidal Pt particles before addition of spacer molecules. The average particle size is 1.3 nm. (b) Same as (a) for cross-linked particles. The average particle size is 1.2 nm.

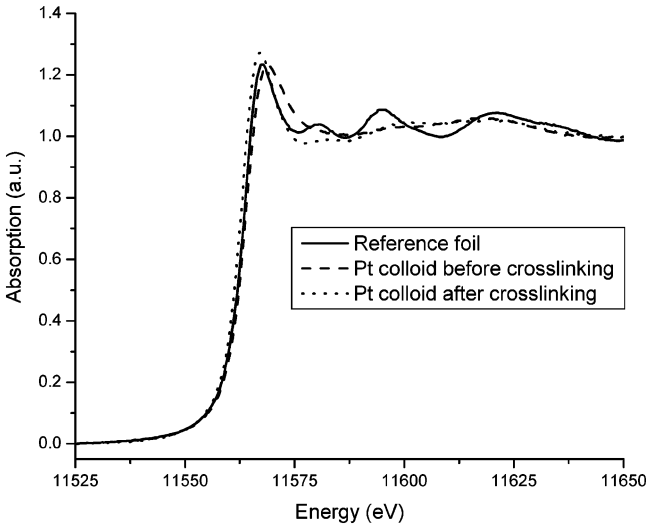

Figure 2. Pt L_{III}-XANES spectra of Pt reference foil (−), and Al-organically stabilized Pt colloid after cross-linking with sebacylic acid (····); the same material before cross-linking (− − − −).

"standard" Pt−O bond is formed, but only a relatively weak, coordinative bond to this type of atom is created. A weaker

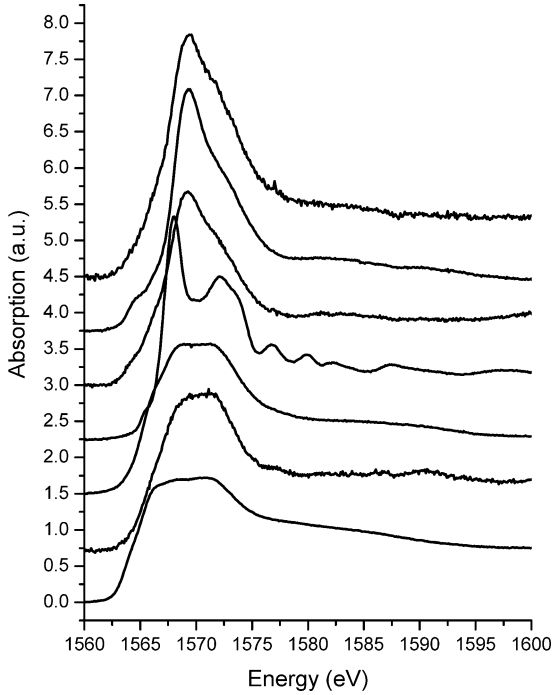

Figure 3. Al K-XANES spectra of (top to bottom): Co colloid, cross-linked with sebacylic acid; Pt colloid, cross-linked with sebacylic acid; Co colloid, cross-linked with a mixture of sebacylic acid and 1-decanol; Al_2O_3; stabilizing shell of Pt colloid; stabilizing shell of Co colloid; aluminiumtrioctyl.

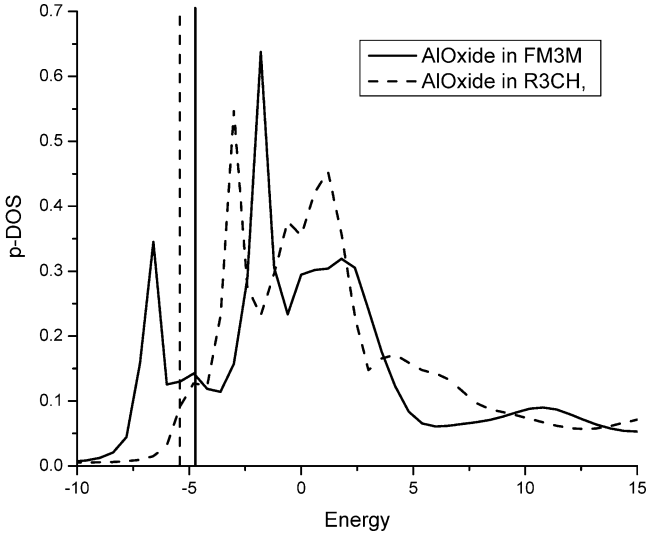

Figure 4. p-projected density of states for AlO clusters in *FM3M* (−) and *R3CH* (− − − −) symmetry, respectively. Straight lines indicate the position of the Fermi energy for the respective systems. Note that the main feature is shifted by almost 2 eV toward higher energies for the octahedrally coordinated Al atoms, reproducing the trend and order of magnitude of the shift observed in the experimental data of the cross-linked particles.

shift in the same direction was observed for different spacer molecules in ref 26, but was of the order of magnitude of the error in energy calibration in that study and thus not interpreted as physical effect.

The key for the ability to interpret the thus-induced changes is obtaining information on the changes within the protection shell, which are induced by the cross-linking process, which can be provided by Al K-edge XANES spectroscopy. The results of such measurements performed on this system are shown in Figure 3 along with a number of reference spectra.

These data show clearly that the networking process using sebacylic acid changes the nature of the aluminumorganic protection shell drastically. Comparing the spectra obtained for aluminumtrioctyl and the one of the aluminumorganically stabilized Pt particle, the partial substitution of octyl groups by acetylacetonate groups is reflected by the gain in white line intensity and a shift of the edge position to higher energy. It is also evident from these spectra that one is not simply dealing with uncontrolled oxidative processes, which in principle should not affect the protection shell due to the handling under protection gas anyway, whose potential effect was simulated by controlled exposure of trimethylaluminide to air (not shown). Even the spectrum of Al_2O_3, which would be accessible from the initial protection shell only via thermal activation, shows a less pronounced white line and is found shifted to lower photon energies relative to the spectrum observed after cross-linking with the acidic spacer. The combination of these two changes implies that the observed changes in the top two spectra in Figure 3 cannot be related to a mere reduction of local order in the networked system as compared to the crystalline Al_2O_3, which would lead to a decreased white line intensity and earlier onset of the absorption edge due to broadening. In any case, position and intensity of the white line hint clearly at a 6-fold coordination of the aluminum atom with strongly electron-drawing ligands. To obtain further information on the local coordination around the Al atoms, real space full multiple scattering calculations were performed on two model systems using the FEFF8 code,[34] which has been used successfully for the detailed interpretation of XANES spectra for crystalline as well as nanoscaled systems.[36−42] We changed the local arrangement of oxygen around the Al atoms from one consistent with the situation encountered in Al_2O_3 (space group *R*3*CH*) to one consistent with octahedral symmetry, as encountered, for example, in space group *FM*3*M*. One should stress that we use these systems only for demonstration of the effect of changes in local coordination symmetry and do not imply that pure aluminumoxide shells are present, which would contradict the networked nature of the samples. Clearly the octahedral symmetry leads to a clear increase of unoccupied p-DOS and shifts the onset of the structure by almost 2 eV to higher energies, as recognized from Figure 4. Further evidence for a characteristic and controlled change in the surfactant shell consists of the fact that an almost identical spectral signature is observed when investigating the Al K-edge of aluminum-organically stabilized Co particles cross-linked using the same spacer molecule. Slight differences can be related to the fact that the latter system does not contain acac-groups in the aluminumorganic shells and thus the Al environment is slightly different. An additional test for the characteristic changes in the Al K-edge spectra upon addition of the acidic spacer molecule is a control experiment, using a mixture of sebacylic acid and 1-decanol, which should lead to a reduced amount of Al-acid coordination. In fact, reduced intensity of the acidic feature is observed in Figure 3.

To investigate the effect of this significant change on the Pt-particle's surfactant shell in detail, Pt EXAFS was analyzed for the two systems. The results are shown in Figure 5and are summarized in Table 1. Pt−Pt distances agree within the error range with each other, whereas a significant reduction relative to the bulk value of 2.77 Å is observed, which can be tentatively related to the extremely small particle size, which also explains part of the significant observed reduction of the coordination number that is often encountered in nanoparticle systems. Further reasons for such a reduction are discussed extensively in the literature.[26,36,43−46] Yet the most important result for this study is that the analysis verifies clearly that an additional soft

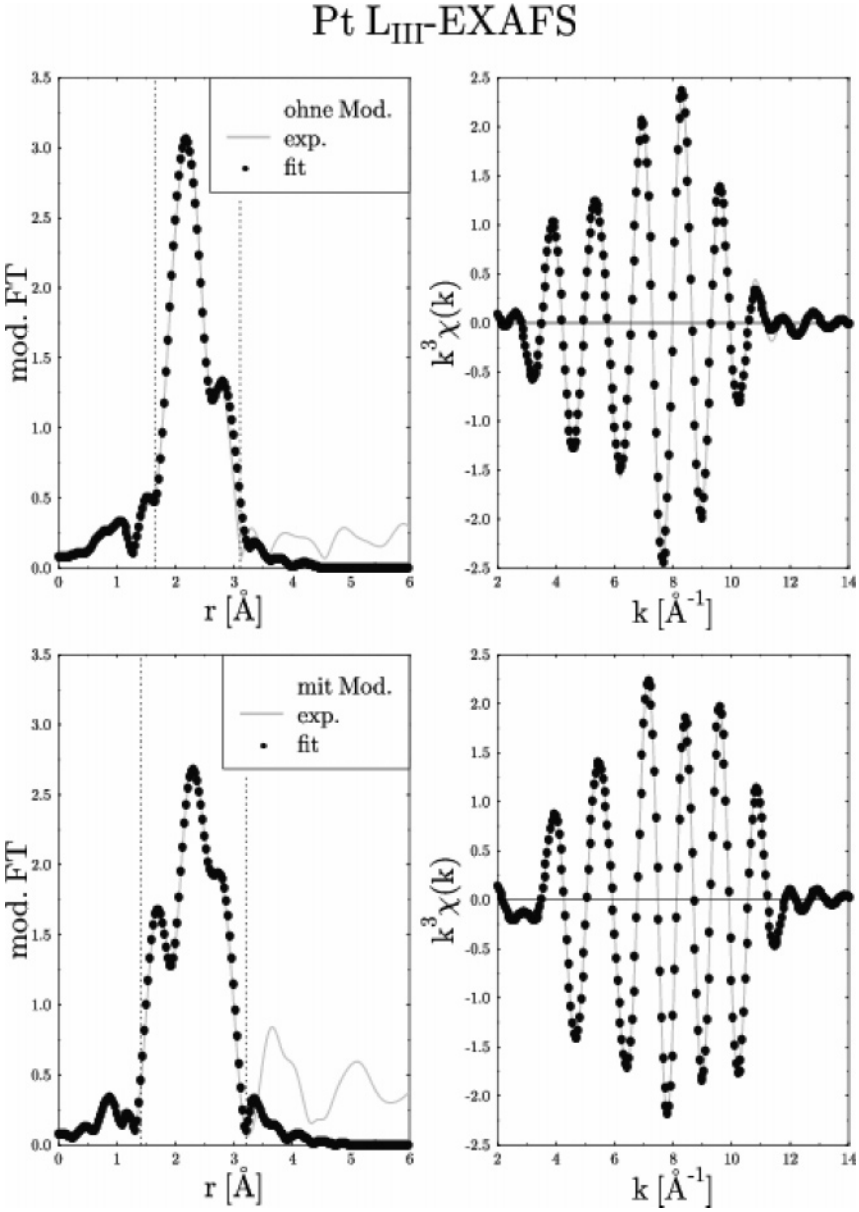

Figure 5. Upper half: k^3-weighted χ(k) function (right panel) and modified Fourier transform (left panel) of Al-organically stabilized Pt colloid before cross-linking. Lines correspond to data, and dots correspond to fitting result. Lower half: As above for the colloid after cross-linking with sebacylic acid.

TABLE 1: Results of Pt L$_{III}$ EXAFS Analysis[a]

Pt L$_{III}$-Kante	backscatterer	R [Å]	N	σ^2 [Å]^2	E_0 [eV]
unconnected	Al	2.48 ± 0.02	0.8 ± 0.4	0.002 ± 0.003	0.1 ± 6.3
	Pt	2.70 ± 0.02	4.0 ± 3.3	0.011 ± 0.006	-0.5 ± 3.6
connected	O	2.07 ± 0.01	0.7 ± 0.1	0.005 ± 0.001	8.1 ± 1.6
	Al	2.53 ± 0.01	0.4 ± 0.1	0.002 ± 0.002	2.9 ± 2.8
	Pt	2.67 ± 0.01	4.7 ± 0.6	0.009 ± 0.001	0.9 ± 0.8

[a] Fitting was done in r-space between 1.5 and 3.2 Å using a k-weight of 3, $S_0^2 = 0.875$.

backscatterer, most likely oxygen, contributes to the signal and leads to a partial substitution of the aluminum as nearest neighbor (see Table 1). It should be pointed out that the total coordination number and the number of first shell Pt neighbors stay identical within the error range and no Pt−Pt scatterers appear at a distance of 3.1 Å, which would be expected for the formation of the platinum-oxide phase. Therefore, one can rule out the possibility that the increased white line intensity is an indicator for the formation of such a phase.

Now, it is rather easy to combine the facts obtained from Al K-end Pt L$_{III}$-edge into one consistent picture, which is schematically presented in Scheme 3: At each Al-site on which cross-linking occurs (note that this is not equivalent for all Al-sites), the oxygen-coordination of the Al atom is changed from 4 in the aluminum-methyl-bisacetylacetonat configuration to 6. Whereas in the first case a planar configuration of the oxygen atoms is possible which allows for a Pt−Al coordination, in the second case the oxygen-cage is three-dimensional, which in turn introduces oxygen as an interfacial layer between Pt and Al, as seen in the EXAFS data. The gain in white line intensity is induced by two reasons: On one hand, the local charge at the Al sites is increased; on the other hand, the partial oxygen

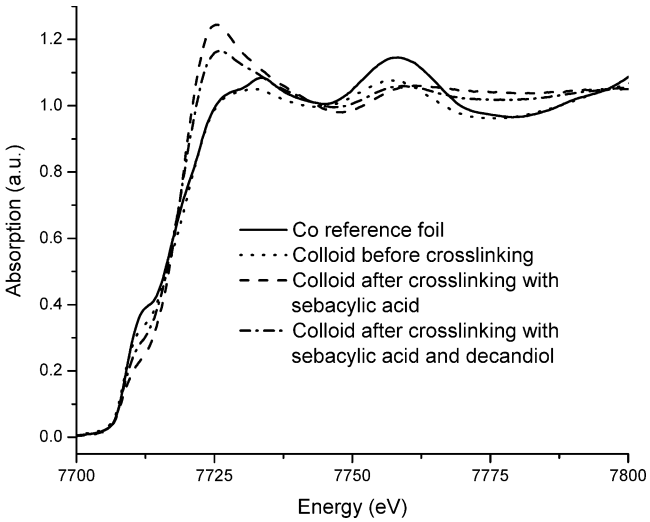

Figure 6. Co K-XANES spectra of Al-organically stabilized Co colloid cross-linked with sebacylic acid (− − − −); the same colloid cross-linked with a mixture of sebacylic acid and decanol (− · − ·); the same colloid before cross-linking (····); hcp Co reference foil (−).

coordination introduces rather electronegative additional binding partners. Both effects act electron-withdrawing at the Pt sites, leading to an increase in unoccupied density of states in the white line region. At the same time, the bond is formed between the Al and the O atom of the spacer-molecule, and this determines the geometry of the entire configuration; thus there is only coordinative interaction between Pt and O, which provides a possible explanation for the unusual shift of the white line to lower energies upon coordination to an electron-drawing partner that is observed in the Pt XANES spectra.

As was already indicated indirectly in the above discussion of the Al K-edge XANES spectra, it is possible to transfer this route to a similar synthesis and networking of reaction molecules to Co nanoparticles. As shown in Figure 6 for a variety of different spacer molecules, also the electronic structure at the Co K-edge as probed by XANES reflects clear and characteristic changes as a function of the spacer molecule employed in the networking process, indicating that this mechanism is more detailed and more general than the singular case discussed above. A more extensive study on the effects of spacer variation is in progress.

Summary and Conclusions

X-ray absorption spectroscopy measurements on both the protection shell and the core of Co and Pt nanoparticles with aluminum-organic stabilizers indicate that connecting such particles with spacer molecules can induce notable changes in the electronic structure of the particle's core. The EXAFS evaluation underlines that this is an effect that leaves the geometric structure of the core of the particle quite unaffected but emerges from the influence of the surfactant shell. Bearing in mind the considerable sensitivity of the properties of nanoparticle cores with respect to the coordination chemistry of the surrounding matrix, the evidence presented here leads to the conclusion that not only is molecular electronics sensitive to the effects of wiring it into a circuit. To achieve working "nanoelectronics" or to functionalize a nanoparticle while conserving its properties, great care has to be taken to avoid changing the designed systems' properties merely by connecting them.

Acknowledgment. Funding by the DFG under contract numbers Mo940 and Bo1135 is gratefully acknowledged.

References and Notes

(1) Reed, M. A.; Zhou, C.; Muller, C. J.; Burgin, T. P.; Tour, J. M. *Science* **1997**, *278*, 252.
(2) Chen, J.; Reed, M. A.; Rawlett, M. A.; Tour, J. M. *Science* **1999**, *286*, 1550.
(3) Collier, C.; Wong, E. W.; Belohradsky, M.; Raymo, F. M.; Stoddart, J. F.; Kuekes, P. J.; Williams, R. S.; Heath, J. R. *Science* **1999**, *285*, 391.
(4) Schon, J. H.; Meng, H.; Bao, Z. *Nature* **2001**, *413*, 713.
(5) Ballardini, R.; Balzani, V.; Clemente-Leon, M.; Credi, A.; Gandolfi, M. T.; Ishow, E.; Perkins, J.; Stoddart, J. F.; Tseng, H. R.; Wenger, S. *J. Am. Chem. Soc.* **2002**, *124*, 12786.
(6) Cui, X. D.; Primak, A.; Zarate, X.; Tomfohr, J.; Sankey, O. F.; Moore, A. L.; Moore, T. A.; Gust, D.; Nagahara, L. A.; Lindsay, S. M. *J. Phys. Chem. B* **2002**, *106*, 8609.
(7) Dunlap, D. D.; Garcia, R.; Schabtach, E.; Bustamante, C. *Proc. Natl. Acad. Sci. U.S.A.* **1993**, *90*, 7652.
(8) Fink, W.; Schoenberger, C. *Nature* **1999**, *398*, 407.
(9) Porath, D.; Bezryadin, A.; de Vries, S.; Dekkar, C. *Nature* **2000**, *403*, 635.
(10) Kasumov, A. Y.; Kociak, M.; Gueron, S.; Reulet, B.; Volkov, V. T.; Klinov, D. V.; Bouchiat, H. *Science* **2001**, *291*, 280.
(11) Vestal, C. R.; Zhang, Z. J. *J. Am. Chem. Soc.* **2003**, *125*, 63.
(12) Torma, V.; Vidoni, O.; Simon, U.; Schmid, G. *Eur. J. Inorg. Chem.* **2003**, 1121.
(13) Link, S.; Furube, A.; Mohamed, M. B.; Asahi, T.; Masuhara, H.; El-Sayed, M. A. *J. Phys. Chem. B* **2002**, *106*, 945.
(14) Mohamed, M. B.; Ahmadi, T. S.; Link, S.; Braun, M.; El-Sayed, M. A. *Chem. Phys. Lett.* **2001**, *343*, 55.
(15) Halte, V.; Bigot, J. Y.; Palpant, B.; Broyer, M.; Prevel, B.; Perez, A. *Appl. Phys. Lett.* **1999**, *75*, 3799.
(16) Zhang, J. Z. *Acc. Chem. Res.* **1997**, *30*, 423.
(17) Diamant, Y.; Chen, S. G.; Melamed, O.; Zaban, A. *J. Phys. Chem. B* **2003**, *107*, 1977.
(18) Rajh, T.; Chen, L. X.; Lukas, K.; Liu, T.; Thurnauer, M. C.; Tiede, D. M. *J. Phys. Chem. B* **2002**, *106*, 10543−10552.
(19) Rabani, E.; Hetenyi, B.; Berne, B.; Brus, L. E. *J. Chem. Phys.* **1999**, *110*, 5355.
(20) Ankudinov, A. L.; Rehr, J. J.; Low, J.; Bare, S. *Phys. Rev. Lett.* **2001**, *86*, 1642.
(21) Hosokawa, H.; Fujiwara, H.; Murakoshi, K.; Wada, Y.; Yanagida, S.; Satoh, M. *J. Phys. Chem.* **1996**, *100*, 6649.
(22) Zhang, P.; Sham, T. K. *Appl. Phys. Lett.* **2002**, *81*, 736.
(23) Zhang, P.; Sham, T. K. *Phys. Rev. Lett.* **2003**, *90*, 245502.
(24) Bucher, S.; Hormes, J.; Modrow, H.; Brinkmann, R.; Waldöfner, N.; Bönnemann, H.; Beuermann, L.; Krischok, S.; Maus-Friedrichs, W.; Kempter, V. *Surf. Sci.* **2002**, *497*, 321.
(25) Modrow, H.; Bucher, S.; Hormes, J.; Brinkmann, R.; Bönnemann, H. *J. Phys. Chem. B* **2003**, *107*, 3684.
(26) Beuermann, L.; Maus-Friedrichs, W.; Krischok, S.; Kempter, V.; Bucher, S.; Modrow, H.; Hormes, J.; Waldöfner, N.; Bönnemann, H. *Appl. Organomet. Chem.* **2003**, *17*, 268.
(27) Bönnemann, H.; Waldöfner, N.; Haubold, H. G.; Vad, T. *Chem. Mater.* **2002**, *14*, 1115.
(28) Bönnemann, H.; Brijoux, W.; Brinkmann, R.; Matoussevitch, N.; Waldöfner, N.; Palina, N.; Modrow, H. *Inorg. Chim. Acta* **2003**, *350*, 617.
(29) Kumar, C. S. S. R.; Aghasyan, M.; Modrow, H.; Doomes, E.; Henk, C.; Hormes, J.; Tittsworth, R. C. *J. Nanopart. Res.* **2004**, *6*, 369.
(30) Thompson, A.; et al. "X-ray Data Booklet", LBNL/Pub-490 Rev. 2.
(31) Stern, E. A.; Newville, M.; Ravel, B.; Yacoby, Y.; Haskel, D. *Physica B* **1995**, *209*, 117.
(32) Newville, M.; Livins, P.; Yacoby, Y.; Rehr, J. J.; Stern, E. A. *Phys. Rev. B* **1993**, *47*, 14126.
(33) Newville, M.; Ravel, B.; Haskel, D.; Stern, E. A.; Yacoby, Y. *Physica B* **1995**, *209*, 145.
(34) Ankudinov, A. L.; Ravel, B.; Rehr, J. J.; Conradson, S. D. *Phys. Rev. B* **1998**, *58*, 7565−7576.
(35) Rothe, J.; Pollmann, J.; Franke, R.; Hormes, J.; Bönnemann, H.; Brijoux, W.; Siepen, K.; Richter, J. *Fresenius' J. Anal. Chem.* **1996**, *355*, 372.
(36) Angermund, K.; Bühl, M.; Endruschat, U.; Mauschick, F. T.; Mörtel, R.; Mynott, R.; Tesche, B.; Waldöfner, N.; Bönnemann, H.; Köhl, G.; Modrow, H.; Hormes, J.; Dinjus, E.; Gassner, F.; Haubold, H. G.; Vad, T.; Kaupp, M. *J. Phys. Chem. B* **2003**, *107*, 7507.
(37) Chen, L. X.; Liu, T.; Thurnauer, M. C.; Csentcits, R.; Rajh, T. *J. Phys. Chem. B* **2002**, *106*, 8539−8546.
(38) Modrow, H.; Bucher, S.; Ankudinov, A.; Rehr, J. J. *Phys. Rev. B* **2003**, *67*, 035123.

(39) Ankudinov, A. L.; Rehr, J. J.; Low, J.; Bare, S. *Phys. Rev. Lett.* **2001**, *86*, 1642−1645.

(40) Gilbert, B.; Frazer, B. H.; Belz, A.; Conrad, P. G.; Nealson, K. H.; Haskel, D.; Lang, J. C.; Srajer, G.; De Stasi, G. *J. Phys. Chem. A* **2003**, *107*, 2839.

(41) Hallmeier, K. H.; Uhlig, I.; Szargan, R. *J. Electron Spectrosc. Relat. Phenom.* **2002**, *122*, 91.

(42) Reich, A.; Panthöfer, M.; Modrow, H.; Wedig, U.; Jansen, M. *J. Am. Chem. Soc*. **2004**, *126*, 14428.

(43) Di Cicco, A.; Berrettoni, M.; Stiza, S.; Bonetti, E. *Phys. Rev. B* **1994**, *65*, 12386.

(44) Di Cicco, A.; Berrettoni, M.; Stiza, S.; Bonetti, E. *Physica B* **1995**, *208/209*, 547.

(45) Babanov, Y. A.; Golovshchikova, I. V.; Boscherini, F.; Haubold, T.; Mobilio, S. *Nucl. Instrum Methods Phys. Res., Sect. A* **1995**, *359*, 231.

(46) Clausen, B. S.; Norskov, J. N. *Catalysis* **2000**, *10*, 221.